



# Zeolite catalyzed hydroarylation of alkenes with aromatic amines under organic ligand-free conditions



Xinzhi Wang<sup>a,b</sup>, Hongli Wang<sup>a,\*</sup>, Kang Zhao<sup>a,b</sup>, Teng Li<sup>a</sup>, Shujuan Liu<sup>a</sup>, Hangkong Yuan<sup>a</sup>, Feng Shi<sup>a,\*</sup>

<sup>a</sup> State Key Laboratory for Oxo Synthesis and Selective Oxidation, Lanzhou Institute of Chemical Physics, Chinese Academy of Sciences, No.18, Tianshui Middle Road, Lanzhou 730000, China

<sup>b</sup> University of Chinese Academy of Sciences, No. 19A, Yuquan Road, Beijing 100049, China

## ARTICLE INFO

### Article history:

Received 24 September 2020

Revised 7 December 2020

Accepted 13 December 2020

Available online 23 December 2020

### Keywords:

Hydroarylation

Zeolite

USY

Amine

Alkene

Hofmann rearrangement

## ABSTRACT

The hydroarylation of alkenes with aromatic amines is recognized as the most atom-economical and straightforward approach to obtain functional aromatic amines, which are versatile building blocks in organic synthesis and material chemistry. However, controllable synthesis of single hydroarylation product is still a significant challenge because hydroarylation reaction often delivers four hydroarylation products and hydroamination products are also produced during the reaction. Herein, we report the first example of heterogeneous zeolite catalyzed hydroarylation of styrene and norbornene with aniline derivatives under organic ligand-free conditions. With the USY zeolite as catalyst, a wide scope of alkenes and aromatic amines with various functional groups are smoothly converted into the corresponding products in 48–95% yields with high regioselectivity. Detailed characterizations revealed that Lewis acid can promote Hofmann-Martius rearrangement of hydroamination products toward hydroarylation products, resulting in high selectivity for hydroarylation products. In addition, it could be found that the weak acid sites of zeolite play a key role in forming hydroarylation products. Furthermore, the catalyst can be reused at least 10 times without obvious deactivation. This work may promote the development of heterogeneous catalyst system for alkene hydroarylation.

© 2020 Elsevier Inc. All rights reserved.

## 1. Introduction

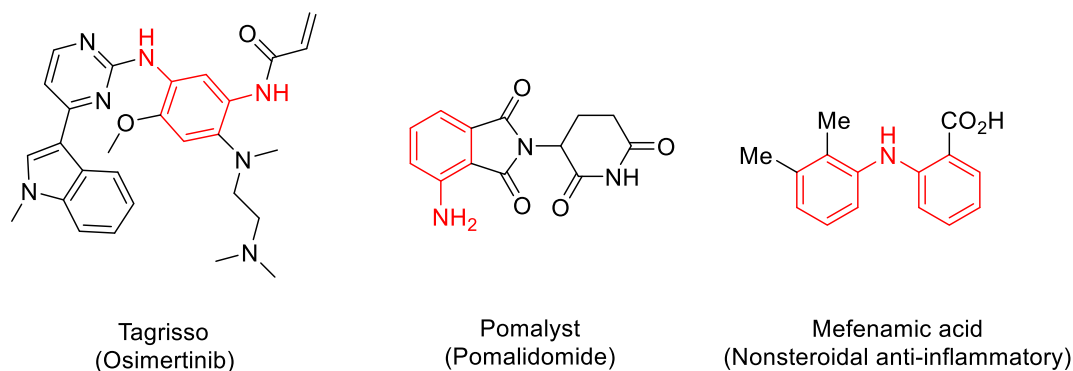
Catalytic hydroarylation of alkenes with aromatic amines is an efficient and 100% atom utilization synthetic route to a variety of functional aromatic amines, which are important structural motifs commonly found in pharmaceuticals, agrochemicals, ligands, fine chemicals and bioactive molecules (Scheme 1) [1]. Traditionally, hydroarylation is accomplished either via classical Friedel-Crafts reaction or through methods based on metal catalyzed C-H activation of arenes [2,3]. The first transition metal-catalyzed hydroarylation of aniline with styrene was reported by Beller and co-workers with [Rh(cod)<sub>2</sub>]<sub>2</sub>BF<sub>4</sub> / 4 mol% PPh<sub>3</sub> and 20 mol% HBF<sub>4</sub>·OEt<sub>2</sub> (Scheme 2a) [4]. Bergman and co-workers identified that HNTf<sub>2</sub> exhibited catalytic activity for the hydroamination/hydroarylation of vinyl arenes and norbornene with anilines at mild temperature (Scheme 2b) [5]. Recently, NaOAc promoted *para*-hydroarylation of  $\alpha$ -methylstyrene with aniline derivatives in hexafluoroisopropanol (HFIP) has been reported by Colomer (Scheme 2c) [6]. Interest-

ingly, Leboeuf found the combination of Ca(NTf<sub>2</sub>)<sub>2</sub> and hexafluoroisopropanol could obtain the *ortho*-C-alkylation products of anilines with alkenes in 35–95% yields [7]. So far, other homogeneous catalysts, such as Ir [8,9], Au [10–12], Ru [13], Co [14], Zn [15], Y [16], Cu [17], Sc [18], nonmetal [19–22] and acid [23–28], have been investigated in hydroarylation of aniline and styrene derivatives. Although the progress in hydroarylation of aniline and styrene derivatives has been made, there is still room for further improving the chemo- and regioselectivity of this reaction. Furthermore, the use of heterogeneous catalyst for hydroarylation of alkenes with aromatic amines is more desirable and attractive owing to the convenience of recovering and recycling of the catalysts. Nevertheless, to the best of our knowledge, no heterogeneous catalyst system for hydroarylation reactions of styrene and norbornene with aniline derivatives has been reported. Thus, it is highly desirable to develop heterogeneous catalyst system for highly chemo- and region-selective hydroarylation reactions.

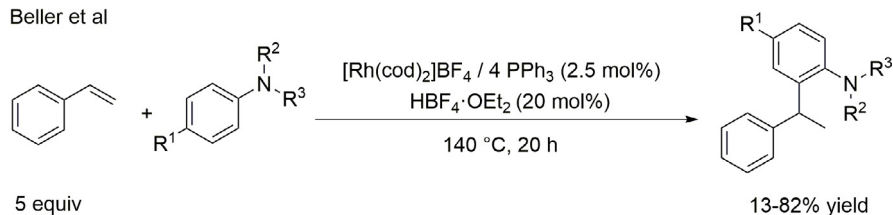
It is well known that zeolites are widely applied in many catalytic transformations in modern organic chemistry owing to their adjustable pore structure and acid type and acid strength [29–37]. For example, ZSM-5 has been successfully used for the amination of isobutylene [38]. It can be attributed to the matching of the pore

\* Corresponding authors.

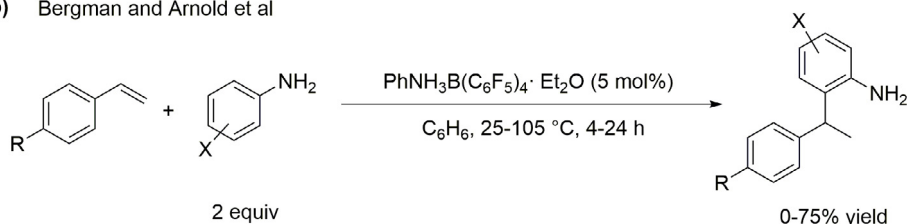
E-mail addresses: [wanghl@licp.cas.cn](mailto:wanghl@licp.cas.cn) (H. Wang), [fshi@licp.cas.cn](mailto:fshi@licp.cas.cn) (F. Shi).

**Scheme 1.** Bioactive molecules containing the aromatic amines structure.**Previous work: homogeneous catalyst system**

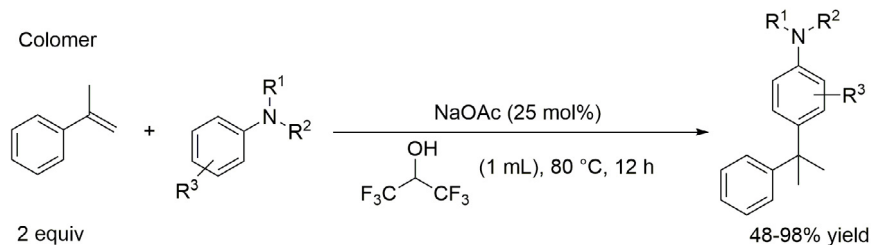
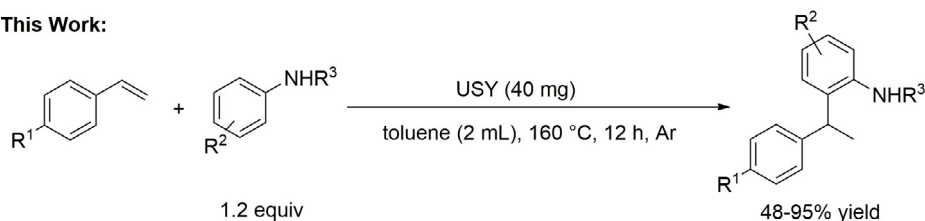
(a) Beller et al



(b) Bergman and Arnold et al



(c) Colomer

**This Work:**

- ✓ High yield and selectivity
- ✓ Easy to recover and recycle
- ✓ Broad substrate scope
- ✓ Organic ligand-free

**Scheme 2.** The hydroarylation of styrene and aniline derivatives.

size of the ZSM-5 and the molecular size of the isobutylene, thereby utilizing the acid sites and effect of zeolite channel [39–41]. Based on the above discussions and our original experience of precisely controlling in catalytic amination selectivity [42–44],

we envisaged that suitable pore size and acid sites of zeolite might be capable of highly selective hydroarylation of alkenes with aromatic amines. Herein, the first example of heterogeneous catalyzed hydroarylation of styrene and norbornene with aniline derivatives

was developed with USY zeolite as catalyst under organic ligand-free conditions (Scheme 2).

## 2. Experimental section

### 2.1. Catalyst preparation

All solvents and chemicals were obtained commercially and used as received.

Zeolites with different structures and different chemical compositions were purchased from different companies. MOR (Si/Al = 25, H type), ZSM-5 (Si/Al = 27, H type), SAPO-11 (Si/Al = 0.5, H type), USY (Si/Al = 11, H type) and USY (Si/Al = 5.4, H type) were purchased from Nankai University Catalyst Co., Ltd.  $\beta$  (Si/Al = 30, H type) was received from Shandong Qilu Huaxin High-Tech Co., Ltd. NaY was purchased from J&K Scientific Ltd. HY was prepared by ion exchange 3 times, NaY in 1 mol/L  $\text{NH}_4\text{NO}_3$  solution (Solid-liquid ratio = 1:20) at 80 °C for 24 h, then calcined at 550 °C for 3 h. All zeolites without special description in this article were calcined for 3 h at a heating rate of 10 °C/min to 550 °C from room temperature.

### 2.2. Catalyst characterization

XRD measurements were conducted by using a STADIP automated transmission diffractometer (STOE) equipped with an incident beam curved germanium monochromator with  $\text{CuK}\alpha_1$  radiation and current of 40 kV and 150 mA, respectively. The XRD patterns were scanned in the 2 Theta range of 5–80°.

The BET surface area measurements were performed on a Quantachrome IQ<sub>2</sub> at the temperature of 77 K. The pore size distribution was calculated from the adsorption–desorption isotherm by using the DFT method. Prior to measurements, the samples were degassed at 300 °C for 3 h, at a rate of 10 °C·min<sup>−1</sup>.

Py-IR spectra of samples were analyzed by a Bruker VERTEX 70 FTIR spectrometer. The samples were weighed and pressed into transparent disk with a diameter of 15 mm. Then, the sample was heated at 400 °C under vacuum for 1 h, and cooled to 150 °C then pyridine was chemisorbed for 10 min. After this step, the sample was evacuated and analyzed by FTIR.

$\text{NH}_3$ -TPD was performed on a chemisorption analyzer equipped with a thermal conductivity detector (TCD). The chemisorption analyzer was TP-5080D from Tianjin Xianquan Industrial and Trading Co., Ltd. The weighed sample (100 mg) was pretreated at 400 °C for 1 h under He (40 mL·min<sup>−1</sup>) and cooled to 100 °C. The  $\text{NH}_3$  gas (30 mL·min<sup>−1</sup>) was introduced instead of He at this temperature for 0.5 h to ensure the saturation adsorption of  $\text{NH}_3$ . The sample was then purged with He for 1 h (40 mL·min<sup>−1</sup>) until the signal returned to the baseline as monitored by a thermal conductivity detector (TCD). The desorption curve of  $\text{NH}_3$  was acquired by heating the sample from 100 °C to 700 °C at 10 °C·min<sup>−1</sup> under He with the flow rate of 40 mL·min<sup>−1</sup>.

<sup>27</sup>Al MAS NMR were carried out on a Bruker AVANCE III 600 spectrometer at a resonance frequency of 156.4 MHz using a 4 mm HX double-resonance MAS probe at a sample spinning rate of 14 kHz. <sup>27</sup>Al MAS NMR spectra were recorded by small-flip angle technique with a pulse length of 0.68  $\mu\text{s}$  ( $<\pi/12$ ) and a 1 s recycle delay. The chemical shift of <sup>27</sup>Al was referenced to 1 M aqueous Al ( $\text{NO}_3$ )<sub>3</sub>.

NMR spectra were measured using a Bruker ARX 400 or ARX 100 spectrometer at 400 MHz (<sup>1</sup>H) and 100 MHz (<sup>13</sup>C).

### 2.3. Typical procedure for hydroarylation of amines and alkenes

A mixture of alkene (1.0 mmol), amine (1.2 mmol), USY (40 mg), toluene (2 mL) were added into a 38 mL press tube and exchanged

with Ar. The reaction was carried out at 160 °C (reaction temperature) for 12 h with a magnetic stirring speed of 500 rpm/min. After the reaction finished, the press tube was cooled to room temperature and 0.5 mmol triphenylmethane was added. Subsequently, the reaction mixture was diluted with 8 mL of methanol and centrifuged. Then, 0.75 mL of the supernatant liquid was taken and treated with hydrochloric acid (12 mol/L, 5–6 drops). Finally, the mixture was concentrated by a rotary evaporator and 0.5 mL  $\text{CDCl}_3$  was added for quantitative analysis by <sup>1</sup>H NMR.

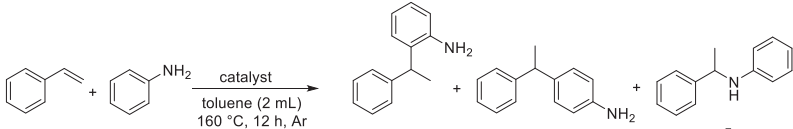
The scale-up experiments were performed in a 100 mL magnetic stirred autoclave equipped with a PID temperature controller. A mixture of styrene (25.0 mmol, 2.6 g), aniline (30.0 mmol, 2.8 g), USY (1.0 g), toluene (50 mL) were added and exchanged with Ar. The reaction was carried out at 160 °C (reaction temperature) for 12 h with a magnetic stirring speed of 500 rpm/min.

## 3. Results and discussion

### 3.1. Screening of different zeolites for hydroarylation of styrene and aniline

In order to verify our conjecture, we selected various zeolites with different structures and morphologies for hydroarylation of styrene and aniline as a model reaction (Table 1). Meanwhile, we calculated the molecular sizes of reactants and products theoretically. It was found that the equivalent diameters of styrene, aniline, 2-(1-phenylethyl)aniline, 4-(1-phenylethyl)aniline and N-(1-phenylethyl)aniline are 8.34 Å, 8.04 Å, 9.94 Å, 9.92 Å and 9.92 Å (Fig. 1). Obviously, the computational results revealed that the pore diameter of the zeolite should be greater than 9.94 Å for the products leaving the pore. Initially, low yields were obtained on the small pore size zeolites for the hydroarylation of styrene and aniline (entries 1–3, Table 1), such as ZSM-5 (Framework Type: MFI, Maximum diameter of a sphere: 6.36 Å [45]), MOR (Framework Type: MOR, Maximum diameter of a sphere: 6.7 Å [45]) and SAPO-11 (Framework Type: AEL, Maximum diameter of a sphere: 5.64 Å [45]). Gratifyingly, a promising yield of 36% was observed when  $\beta$  (Framework Type: BEA, Maximum diameter of a sphere: 6.68 Å [45]) was used, but selectivity for hydroamination was 58% (entry 4, Table 1). Then, we systematically investigated the performance of Y-type zeolite (Framework Type: FAU, Maximum diameter of a sphere: 11.24 Å [45]). When using NaY, 5% yield and 40% selectivity for hydroarylation could be obtained (entry 5, Table 1). Surprisingly, the yield and the selectivity of hydroarylation were improved after ion exchange 3 times (entry 6, Table 1). To our delight, USY (Si/Al = 11) significantly increased the yield and selectivity to 68% (entry 7, Table 1). As the Si/Al ratio decreased to 5.4 and there was no pretreatment of USY, the yield and hydroarylation selectivity were 65% and 68%, respectively (entry 8, Table 1). With the increase in the calcination temperature of USY, such as USY(5.4)-400 (Si/Al = 5.4, calcination temperature = 400 °C), USY(5.4)-550 (Si/Al = 5.4, calcination temperature = 550 °C), USY(5.4)-800 (Si/Al = 5.4, calcination temperature = 800 °C), the yield can be up to 82% and no hydroamination product was observed (entries 9–11, Table 1). Noteworthy, hydroamination products will be observed when the reaction temperature decreased (entry 12, Table 1) but not at high temperature (entry 13, Table 1). The impact of the solvent on the reactivity of this reaction was further investigated, and it was found that toluene was the optimal choice (Table S1). Meanwhile, the volume of toluene and the amounts of USY were also optimized (Table S2 and S3), and 2 mL toluene and 40 mg USY were proved to be the optimal. It should be noted that the catalyst can be reused at least 10 times without apparent deactivation (entry 14, Table 1).

**Table 1**  
Screening of zeolite catalysts for the hydroarylation of styrene with aniline<sup>a</sup>.

				
Entry	Catalyst (Si/Al)	Yield <sup>b</sup> (%)	3:4:5 <sup>b</sup>	
1	MOR	2 <sup>c</sup>	–	
2	ZSM-5	trace <sup>c</sup>	–	
3	SAPO-11	2	50:0:50	
4	β	36	28:14:58	
5	NaY	5	40:0:60	
6	HY	22	55:13:32	
7	USY (11)	68	68:14:18	
8 <sup>d</sup>	USY (5.4)	65	68:15:17	
9	USY (5.4)-400	76	75:16:9	
10	<b>USY (5.4)-550</b>	<b>82 (81)<sup>e</sup></b>	<b>85:15:0 (88:12:0)<sup>e</sup></b>	
11	USY (5.4)-800	82	85:15:0	
12 <sup>f</sup>	USY (5.4)-550	61	74:8:18	
13 <sup>g</sup>	USY (5.4)-550	81	86:14:0	
14 <sup>h</sup>	USY (5.4)-550	81	85:15:0	

a. Reaction conditions: styrene (1 mmol), aniline (1.2 mmol), catalyst (40 mg), toluene (2 mL), 160 °C, 12 h, argon atmosphere; b. Determined by <sup>1</sup>H NMR using triphenylmethane as internal standard; c. Determined by GC–MS; d. Catalyst without any pretreatment; e. Isolated yield; f. 140 °C; g. 180 °C; h. Reused 10 times.

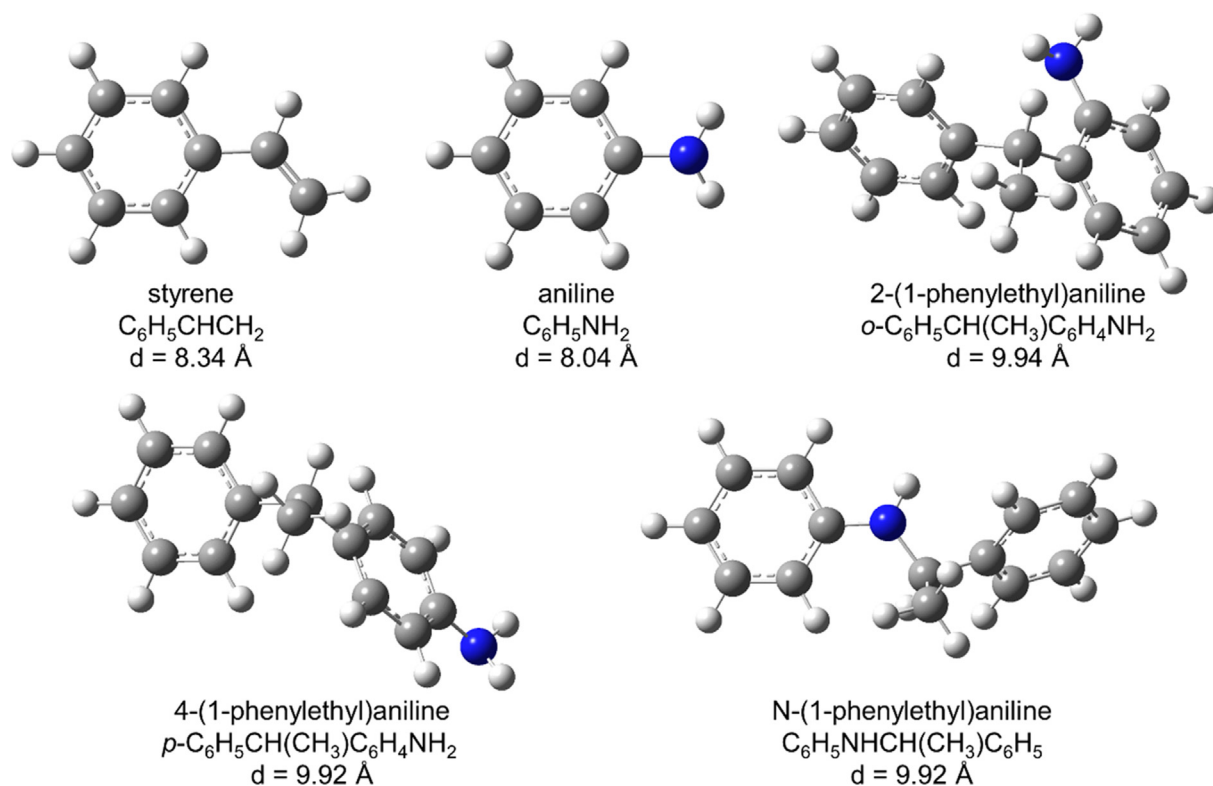


**Fig. 1.** Structures of styrene, aniline, 2-(1-phenylethyl)aniline, 4-(1-phenylethyl)aniline and N-(1-phenylethyl)aniline. Note: All calculation were performed via Gaussian 16 [46] with B3LYP functional [47–50] and 6–31++G(d,p) basis sets [51–53]. d is the equivalent diameter of the largest included sphere.

### 3.2. Characterization of different zeolites

Next, the physical properties of different zeolites were analysed by the N<sub>2</sub> adsorption–desorption analysis, including surface area, pore volume and pore size. The pore size distributions of zeolites were calculated using density functional theory (DFT) method. As shown in Table 2 and Fig. S1, the pore radius of USY is mainly 0.58 nm and the BET surface area is 782.76–886.93 m<sup>2</sup>/g (entries 7–11, Table 2), which is the largest pore size and largest surface

area of all zeolites used. Obviously, high yield was obtained when the pore radius larger than 0.5 nm, and the pore radius of zeolite smaller than 0.5 nm might prevent molecules from entering or exiting from the channel, so the pore size could be utilized to increase the activity of the hydroarylation. The above results demonstrated that large pore size played a key role and was favorable for hydroarylation of styrene and aniline.

In order to reveal the structure and morphology of the zeolites, the samples were further characterized by X-ray diffraction (XRD)

**Table 2**

The physical properties of different zeolites.

Entry	Catalyst	SA (m <sup>2</sup> /g) <sup>a</sup>	PV (cm <sup>3</sup> /g) <sup>a</sup>	R <sub>DFT</sub> (nm) <sup>a</sup>	APR (nm) <sup>a</sup>
1	MOR	534.32	0.33	0.45	1.25
2	ZSM-5	412.99	0.28	0.39	1.33
3	SAPO-11	207.52	0.48	0.35	4.60
4	β	693.05	0.47	0.51	1.35
5	NaY	698.37	0.53	0.45	1.53
6	HY	697.87	0.55	0.56	1.59
7	USY (11)	886.93	0.55	0.58	1.23
8	USY (5.4)	808.27	0.41	0.58	1.01
9	USY (5.4)-400	803.75	0.44	0.58	1.11
10	USY (5.4)-550	786.21	0.51	0.58	1.30
11	USY (5.4)-800	782.76	0.48	0.58	1.22
12	USY (5.4)-550 Reused	817.82	0.56	0.58	1.38

a. Determined by an IQ2 automated gas sorption analyser. SA: surface area; PV: pore volume; R<sub>DFT</sub>: pore radius, pore size distributions of zeolites were calculated using density functional theory (DFT); APR: average pore radius.

and scanning electron microscope (SEM). The XRD patterns for different zeolites are described in Fig. 2. As shown in Fig. 2, the peaks of MOR (JCPDS: 47–0410), ZSM-5 (JCPDS: 44–0003), SAPO-11 (JCPDS: 41–0023), β (JCPDS: 47–0183) and Y-type (JCPDS: 88–2288) zeolites could be observed in the corresponding samples. The SEM images of different zeolites are shown in Fig. 3 and Fig. S2. It can be seen that the morphological features of USY zeolites were similar (Fig. 3 e–i), which means that the calcination did not destroy the structure of USY.

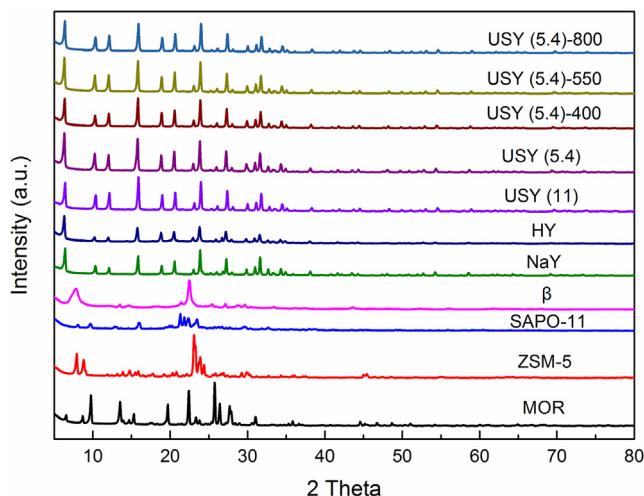
The above results indicated that the improvement in the selectivity stems from the calcination of USY zeolite rather than the structure and morphology of USY zeolite. Therefore, we conducted a systematic study on the acid type and acid strength of different zeolites through Py-IR and NH<sub>3</sub>-TPD. Py-IR shows the amount of Brønsted acid sites and Lewis acid sites, as shown in Fig. 4, Table S5 and Fig. S3. It is well known that the absorption peak at 1450 cm<sup>−1</sup> is assigned to the Lewis acid sites and the absorption peak at 1540 cm<sup>−1</sup> is assigned to the Brønsted acid sites [54,55]. From NaY to HY, the ratio of L/B (Lewis acid / Brønsted acid) decreased from 25.64 to 0.66 (entries 5–6, Table S5), but the yield and selectivity of the hydroarylation reaction increased significantly. These results suggested that the increase in the amount and proportion of B acid was beneficial to hydroarylation reaction, and could also be verified from USY (entries 7–8, Table S5). Interestingly, the amount of L acid in USY increased with increasing calcination temperature, which obviously prevents the formation of

hydroamination products during the reaction (entries 8–11, Table S5). Therefore, it can be inferred that amount of L acid might affect the selectivity of hydroarylation reaction. It is worth noting that the acid type, acid amount and L/B ratio of USY (5.4)-550, MOR and ZSM-5 are similar (entries 1–2 and 10, Table S5), but the highest catalytic performance was obtained by USY. This also illustrates that the large pore size of USY allows raw materials and products to enter and exit freely in the pore.

In order to study the effect of calcination increasing the amount of L acid, we performed FT-IR spectroscopy (Fig. 5) to study the changes in functional groups on the surface of USY (5.4) zeolites. FT-IR spectroscopy showed that the peak at 1401 cm<sup>−1</sup> disappeared after calcining USY (5.4) catalyst. It is known that 1401 cm<sup>−1</sup> peak can be associated to NH bending vibration. This suggests that calcination could desorb the weak NH<sub>4</sub><sup>+</sup> complex as bound to Al or Si [56]. Therefore, more L acid sites are exposed to improve catalytic activity. In addition, the FT-IR results of USY calcined at different temperature are almost the same, but the catalytic performance is different. It can be attributed to the higher temperature that can desorb the weak NH<sub>4</sub><sup>+</sup> complex in the pore, which further proves that the pore of the zeolite is effective in hydroarylation.

The acid strength of the zeolites with different structures were measured by NH<sub>3</sub>-TPD technique and the results were shown in Fig. 6. Obviously, the acid strength of ZSM-5, USY (11) and USY (5.4) are similar, while the poor hydroarylation performance of ZSM-5 can be also attributed to the small pore size. Surprisingly, as the calcination temperature of USY increases, the number of strong acid sites has decreased significantly, while the selectivity of the hydroarylation reaction gradually increases. It can be inferred that strong acid sites inhibit the formation of hydroarylation products. In addition, the amount of weak and strong acid sites in USY (5.4) were quantified (entries 8–11, Table S6). Obviously, calcination reduced the total acid site concentration of USY, but the proportion of weak acid sites increased. Combining the Py-IR results (entries 8–11, Table S5) and TPD data, we could draw conclusion that L acid sites correspond to the weaker acid sites. In brief, the large pore size and surface area of USY, a certain proportion of L/B acid and weak acid sites, promote the hydroarylation reaction of styrene and aniline with complete hydroarylation selectivity.

<sup>27</sup>Al MAS NMR was utilized to investigate whether calcination would cause USY to form extraframework Al debris due to steaming effects (Fig. 7). For the USY after calcination at 550 °C, three maxima were observed at 62, 32, and 2 ppm, which could be assigned to 4-, 5-, and 6-coordinated Al species [57,58]. Compared with pristine USY (5.4), a new signal for 5-coordinated Al species was observed in USY (5.4) calcination at 550 °C. These results indi-

**Fig. 2.** XRD images of the samples.



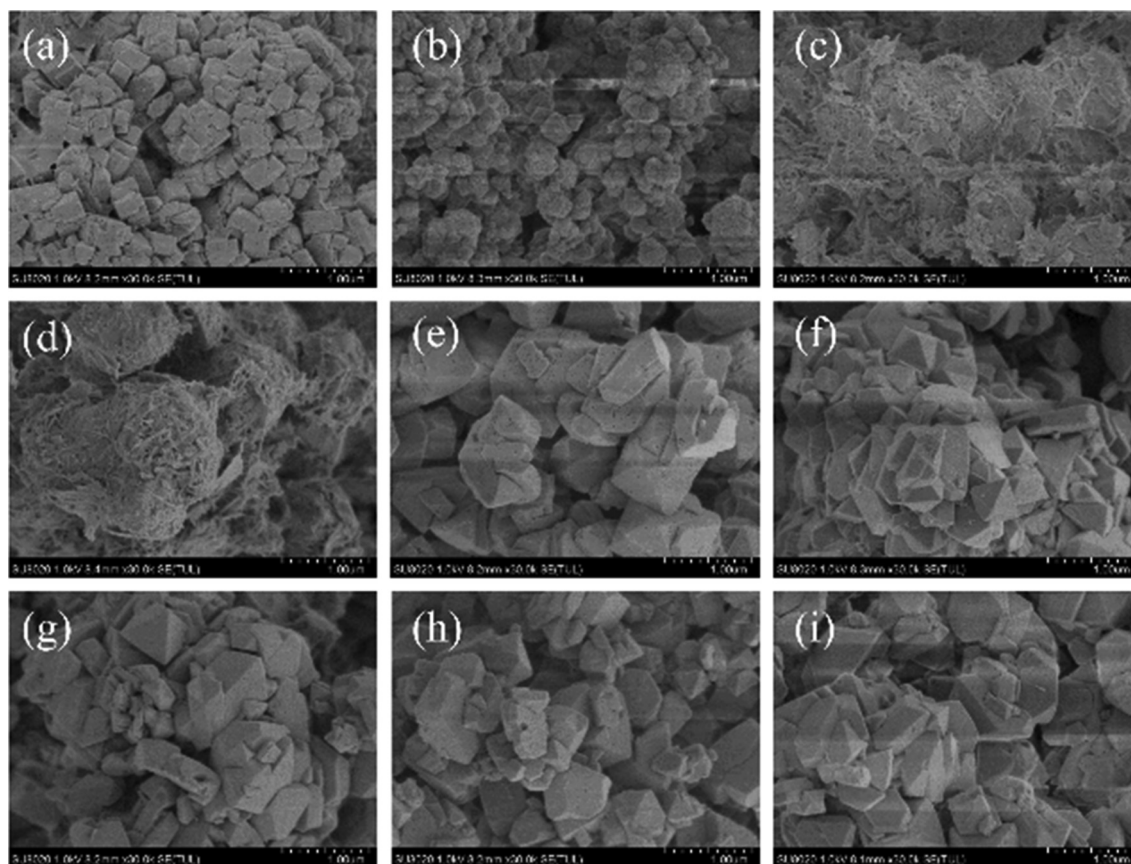


Fig. 3. SEM images of the zeolites. (a) ZSM-5, (b)  $\beta$ , (c) NaY, (d) HY, (e) USY (11), (f) USY (5.4), (g) USY (5.4)-400, (h) USY (5.4)-550, and (i) USY (5.4)-800.

cated that calcination exposed USY to form extraframework Al debris and increased the coordination number of Al. According to the comparison of Py-IR and  $^{27}\text{Al}$  MAS NMR, the increase of L acid caused by calcination might be related to the increase of 5-coordinated Al species. Furthermore,  $^{27}\text{Al}$  MAS NMR showed that no obvious differences were observed upon comparing the fresh and used USY (5.4)-550. In addition, the heating rate of USY was also studied. It was found that low heating rate ( $2^\circ\text{C}/\text{min}$ ) would lead to slightly lower selectivity, while high heating rate ( $\geq 5^\circ\text{C}/\text{min}$ ) would lead to high selectivity (Table S7). It was obvious from the  $^{27}\text{Al}$  MAS NMR data (Fig S7) that this was due to the high selectivity caused by the increased presence of 5-coordinated Al species. Therefore, USY can be modified by the calcination temperature and heating rate, resulting in changes of catalytic performance.

### 3.3. Substrate scope of hydroarylation reaction

With the optimized conditions in hand, the substrate scope and limitation of this catalyst system was further investigated, as shown in Table 3. It was worth mentioning that the reaction is highly selective and only hydroarylation product was observed in most of cases. Initially, we checked the generality of the different primary and secondary amines. Electron-withdrawing and electron-donating groups including *ortho*-, *meta*- and *para*-substituted, such as chlorine and methyl, were all suitable for this transformation, affording the desired products in 56–84% yields (7a–7g). The slight decrease in the yield of *ortho* and *para* groups could be attributed to steric hindrance. Moreover, with electron-rich *n*-butyl, methyl-, methoxy and cycloalkyl substituted aniline as starting materials, moderate to good yields (7h–7o, 54–88%) were achieved. In addition, secondary amines could also proceed

smoothly, giving the corresponding products in 66–95% yields (7p–7t). Notably, when the tetrahydroquinoline derivatives were used as the reactants, the yield and selectivity of the reaction were excellent (7q and 7r, 90 and 95%).

Next, reactions of aniline with different alkenes were examined (Table 4). For example, alkenes with electron-withdrawing group bearing fluoro, chloro and bromine also proceeded well, affording their corresponding products in 48–80% yields (9a–9f). Meanwhile, it was observed that the yields of *ortho*-group alkenes decreased with the weakening of the electronic effect (9d–9f). Alkenes with electron-donating groups such as methyl, *tert*-butyl, methoxy and phenyl, gave the corresponding product in 86–96% yields with the regioselectivity of 21:49–58:42 (9g–9j). In addition, the reaction of *trans*- $\beta$ -methylstyrene, as an example of internal alkene substrate, provided the corresponding product in 51% yield (9k). Furthermore, when indene and aniline underwent a hydroarylation reaction, 86% yield and 49:51 regioselectivity could be obtained (9l). The reaction of 2-vinylthiophene and aniline was also tolerated (9m). Interestingly, 81–88% yields of the *para*-hydroarylation products were obtained when  $\alpha$ -methylstyrene was used as substrate (9n and 9o). The *para*-product yields were similar to that reported in the literature recently [6] and this *ortho*-to-*para* transition can be attributed to the steric hindrance of  $\alpha$ -methylstyrene. Moreover, the recently published work also used DFT calculations to prove that electron-rich olefins might involve different mechanisms and the energy for the *para*-alkylation transition state is higher [7].

At last, the hydroarylation reaction was also performed using norbornene as a substrate in order to investigate the properties of aliphatic alkenes (Table 5). In general, the anilines with both electron-withdrawing and electron-donating groups on the phenyl

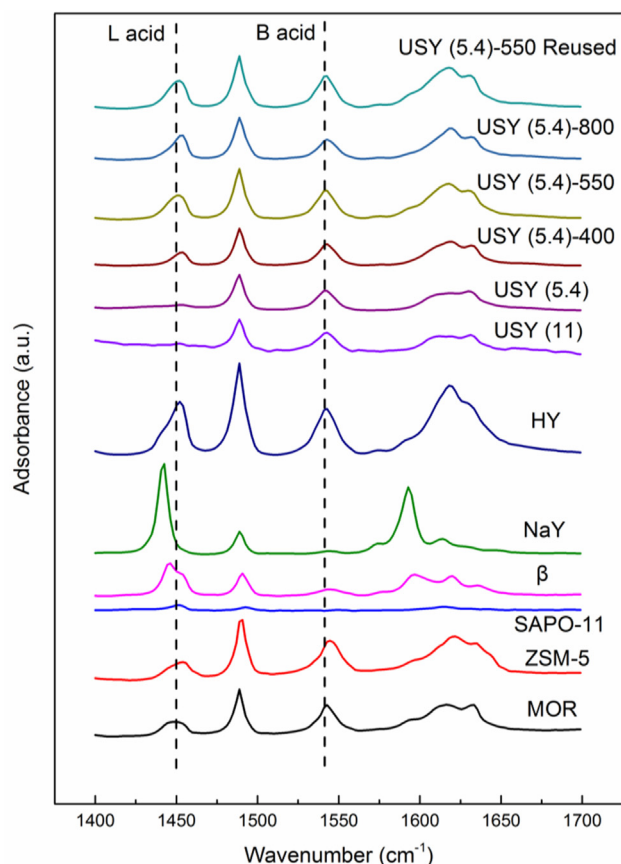


Fig. 4. In situ pyridine-FTIR spectra of the different zeolites.

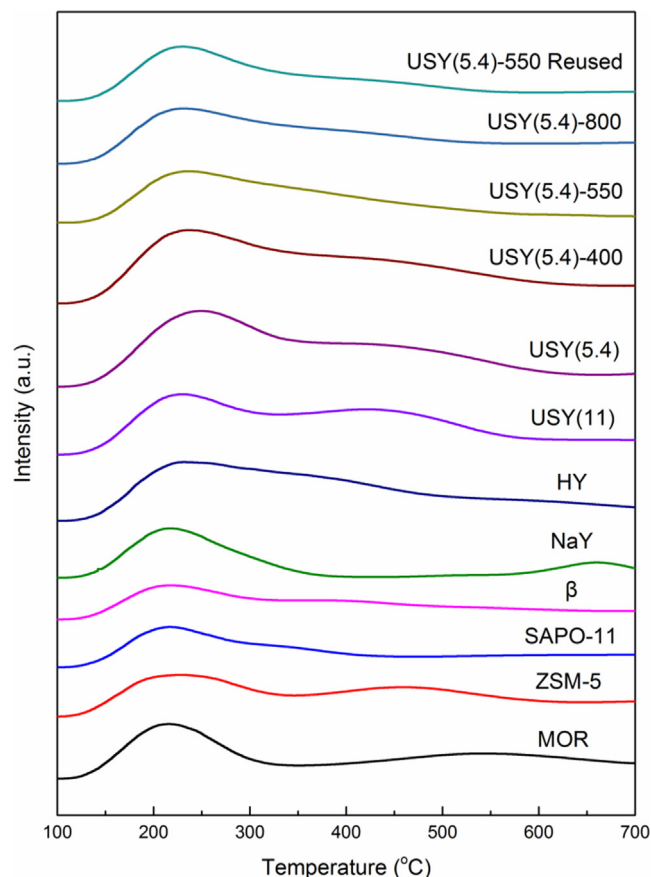


Fig. 6. The  $\text{NH}_3$ -TPD profiles of the different zeolites.

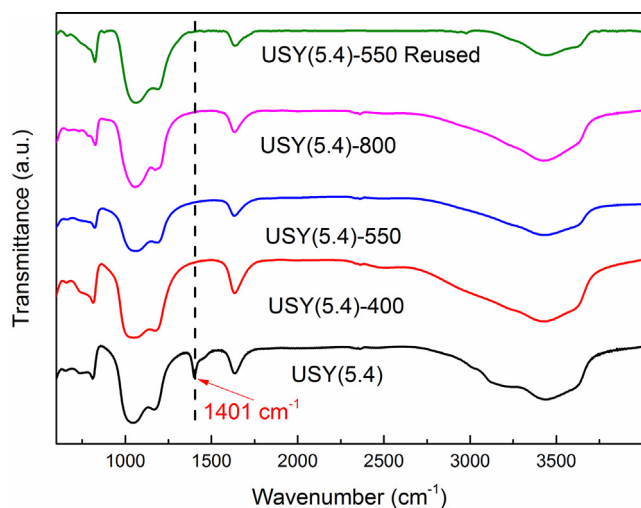


Fig. 5. The FT-IR spectra of the USY zeolites.

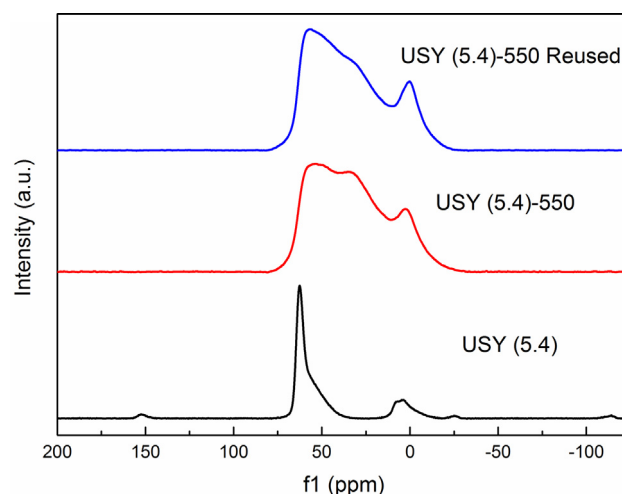


Fig. 7.  $^{27}\text{Al}$  MAS NMR spectra of USY.

ring were well tolerated under the current conditions (entries 1–4, Table 5). It was worth noting that there were some hydroamination products in the reaction, and the selectivity of the hydroarylation products also changed regularly with the strength of the electronic effect. It also can be concluded that amine compounds with electron-donating groups are beneficial to the hydroarylation of norbornene. Moreover, the difference in the ortho–para selectivity between norbornene and styrene hydroarylation products may be caused by differences in the stabilities of protonated intermediates [5]. Unfortunately, no conversion was observed when aliphatic

alkenes, i.e., 1-octene and 1-dodecatylene, were used as the substrates.

### 3.4. Catalytic reaction mechanism

In the process of optimizing the reaction conditions, we selected 6 points to study the relationship between NMR yield and reaction time (Fig. 8 and Table S4) in order to study the reaction mechanism. In the first 9 h of the reaction, we observed a small amount of hydroamination products not exceeding 10% and then gradually

**Table 3**  
USY-catalyzed hydroarylation of styrene with aniline derivatives<sup>a</sup>.

 7a Yield: 84%	 7b Yield: 82%	 7c Yield: 64%	 7d Yield: 56%
 7e Yield: 83%	 7f Yield: 64%	 7g Yield: 79%	 7h [b] Yield: 88%
 7i Yield: 89%	 7j Yield: 75%	 7k Yield: 58%	 7l [c,d] Yield: 54%
 7m [b] Yield: 54%	 7n Yield: 75%	 7o [c] Yield: 85%	 7p Yield: 72%
 7q Yield: 90%	 7r Yield: 95%	 7s [c] Yield: 73%	 7t [b] Yield: 66%

<sup>a</sup> Reaction conditions: Alkenes (1.0 mmol), amines (1.2 mmol), USY (40 mg), toluene (2.0 mL), 160 °C, 12 h, argon atmosphere. Isolated yield. <sup>b</sup> USY (60 mg). <sup>c</sup> 24 h.

disappeared. Therefore, we suspect that the reaction has undergone a Hofmann-Martius rearrangement [59]. In order to verify whether the reaction undergoes Hofmann-Martius rearrangement, a control experiment was conducted under the same conditions. As shown in Scheme 3, hydroamination product completely converted into hydroarylation products with 66% yield, and we also observed 3% aniline yield through GC–MS. These results can fully illustrate part of the hydroarylation of styrene and aniline catalyzed by USY zeolite undergoes Hofmann-Martius rearrangement. Moreover, kinetic experiment revealed a first-order dependence on styrene concentration (Fig S4a), and the amine was found to react slowly and seemed a zero-order reaction (Fig S4b). In addition, the amount of catalyst played an important role in the reaction (Fig S4c) and the productivity of catalyst was the highest with 80 mg USY.

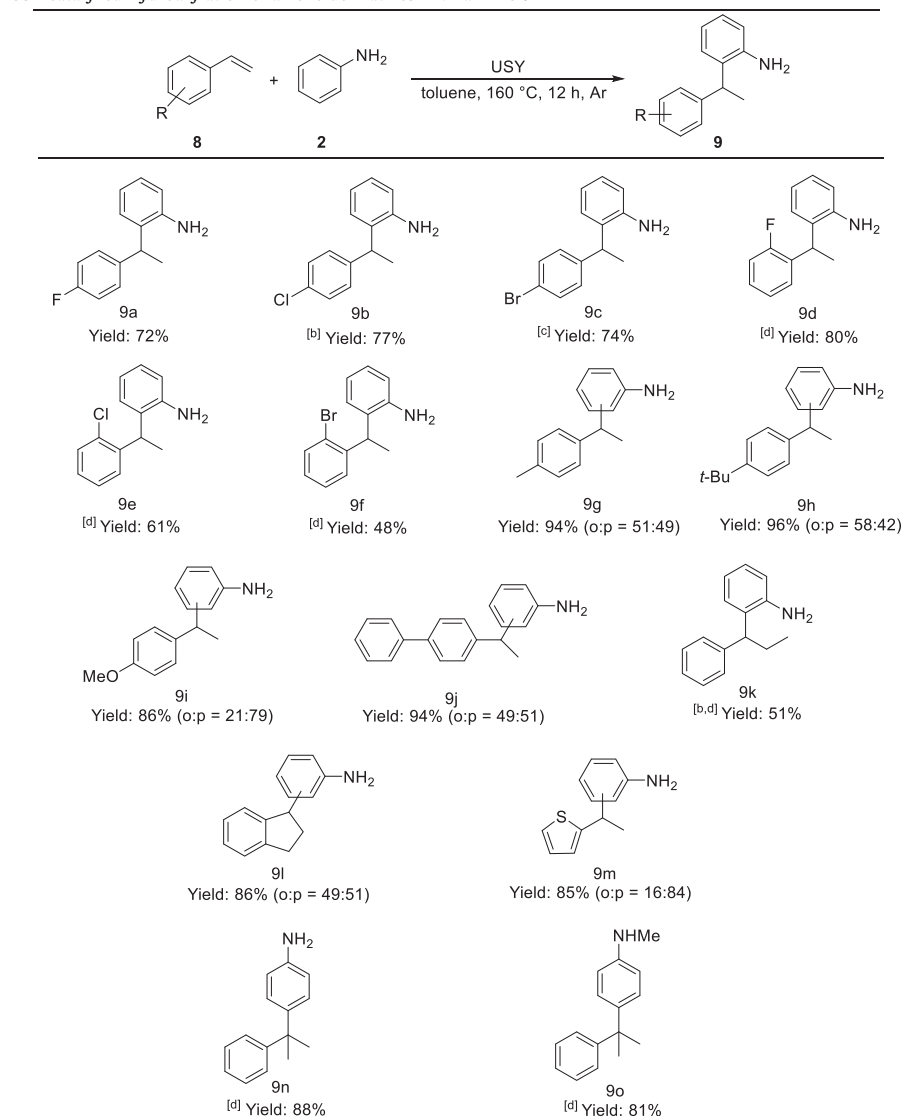
On the basis of the observed experimental results and published literature about dual site/metal catalysis [60–62], a plausible mechanism of this transformation was proposed (Fig. 9). Initially, the protic hydrogen of the acid sites in the zeolite protonates alkenes to generate a carbocation intermediates A [63]. Then, nucleophilic attack of the double bonds in aromatic ring affords the

intermediates B. Subsequent loss of proton and rearrangement of double bond affords the hydroarylation product and regenerate the USY zeolite catalyst for the next catalytic cycle [19]. Meanwhile, nucleophilic attack of the lone electron pair at the aniline nitrogen atom leads to the intermediates B'. Subsequent loss of proton produces the hydroamination product and regenerate the USY zeolite catalyst [5]. With the extension of reaction time and the presence of L acid sites, the hydroamination products undergo a Hofmann-Martius rearrangement leading to complete hydroarylation selectivity.

### 3.5. Scale-up experiment


To highlight the practical utility of this procedure for the synthesis of hydroarylation products, we conducted gram-scale reactions under the similar conditions. The hydroarylation of styrene with aniline on a 25 mmol scale in the presence of 1 g of USY proceeded smoothly at 160 °C for 12 h and afforded the corresponding products in 84% NMR yield with 87:13 selectivity (Scheme 4). These results showed the good chemoselectivity of this catalytic



**Table 4**  
USY-catalyzed hydroarylation of alkene derivatives with aniline<sup>a</sup>.

<sup>a</sup> Reaction conditions: Alkenes (1.0 mmol), amines (1.2 mmol), USY (40 mg), toluene (2.0 mL), 160 °C, 12 h, argon atmosphere. Isolated yield. Regioselectivity was determined by the yield of isolated. <sup>b</sup> USY (60 mg). <sup>c</sup> 180 °C. <sup>d</sup> 24 h.

**Table 5**  
USY-catalyzed hydroarylation of norbornene with aniline derivatives<sup>a</sup>.

				
10 Entry	11	R	Yield/%	12:13
1		H	80	60:40
2		F	84	62:38
3		Me	80	74:26
4		NO <sub>2</sub>	90	10:90

<sup>a</sup> Reaction conditions: Alkenes (1.0 mmol), amines (1.2 mmol), USY (40 mg), toluene (2.0 mL), 160 °C, 12 h, argon atmosphere. Isolated yield. Selectivity was determined by the yield of isolated.

system. Importantly, this result is almost the same as the result of the micro-reaction, so the influencing factors such as utilization

space of the reactor, mass and heat transfer could be ignored under the condition of small dose.

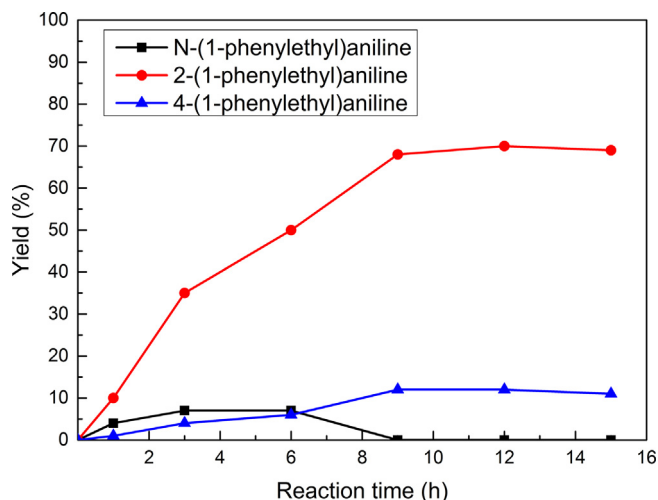


Fig. 8. The relationship between NMR yield and reaction time.

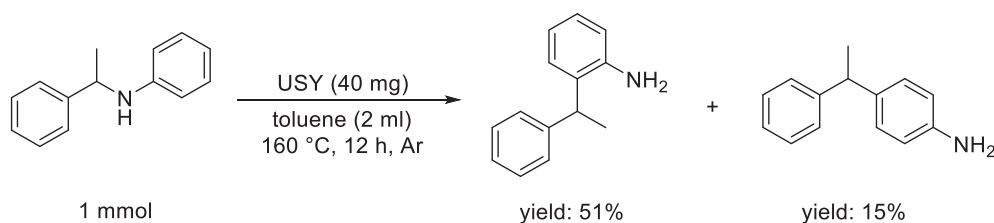
### 3.6. Catalyst recycling experiment

In addition, the reusability of USY was studied (Fig. 10). If the catalyst was used without any treatment for reusability, conversion and selectivity will decrease slightly. The reason might be

attributed to the adsorption of a small amount of amine components and carbon deposition on the surface of catalyst. To improve the reusability, the catalyst was filtered and dried at 80 °C for 6 h, then calcinated for 3 h at 550 °C under an ambient atmosphere after each test, and the performance could be obviously improved after the calcination treatment. To our delight, the catalyst could be reused at least 10 times without loss of activity. The recyclability of the catalyst has also been performed at relatively low conversions within kinetic region, and it can be found that the catalyst could be reused at least 10 times without obvious deactivation (Fig. S5). Moreover, we found that the structure and acidity of the recycled catalyst did not change significantly through characterization (Fig S1, S2, S6 and Figs. 4, 5, 6, 7).

## 4. Conclusion

In conclusion, we have developed the first heterogeneous catalyzed hydroarylation of styrene and norbornene with aniline derivatives under organic ligand-free conditions. By simply calcining USY zeolite, the shape-selective catalyst showed excellent performance in hydroarylation selectivity. A series of hydroarylation products (40 examples, up to 95% yield) were synthesized by applying this simple catalyst system. The N<sub>2</sub> adsorption-desorption results indicated that the suitable pore size of zeolite (pore radius greater than 0.5 nm) facilitated reactants enter and products



Scheme 3. Hofmann-Martius rearrangement.

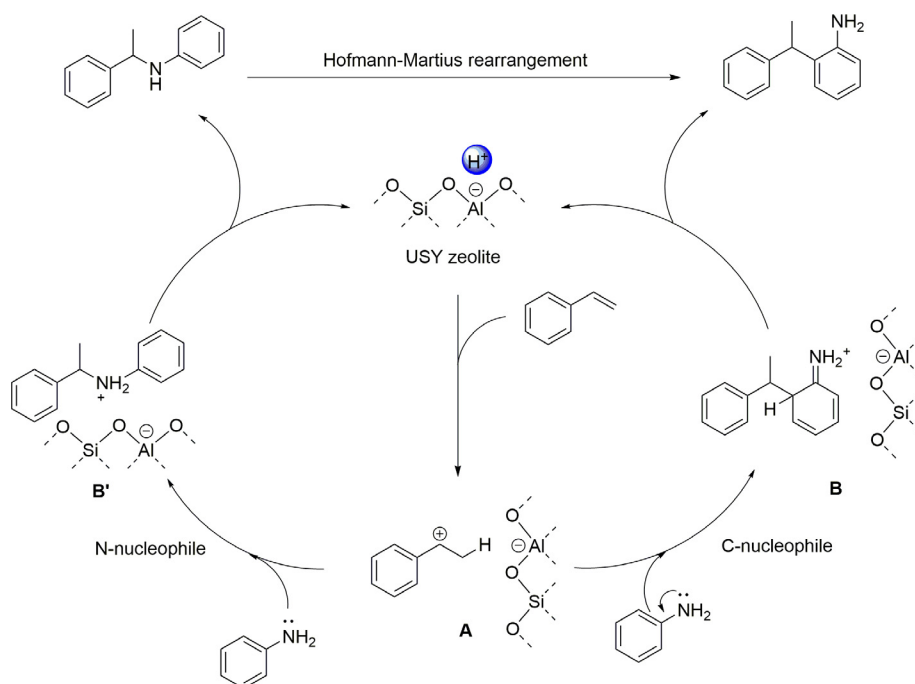
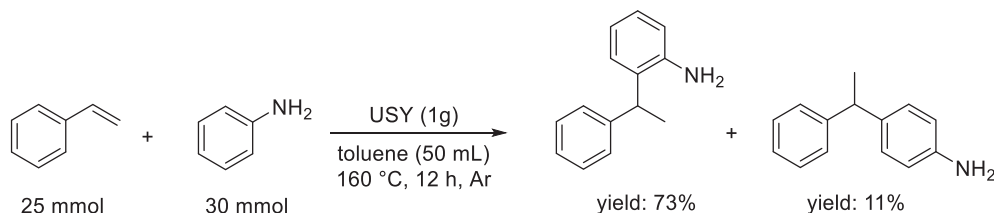


Fig. 9. The proposed catalytic mechanism for hydroarylation of styrene with aniline.



Scheme 4. Gram-scale reaction of styrene with aniline.

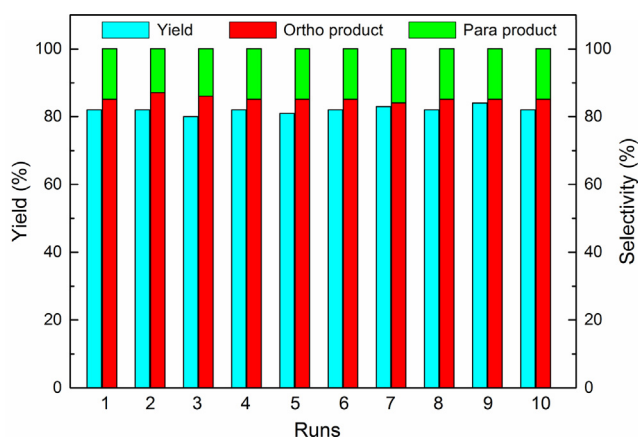


Fig. 10. Recycle test of USY for the hydroarylation of styrene and aniline. (Conditions: styrene 1.0 mmol, aniline 1.2 mmol, USY 40 mg, 160 °C, 12 h, argon atmosphere, 500 rpm/min.)

exit in the pore, thus exhibiting good shape-selectivity. Utilizing Py-IR, it could be proved that Lewis acid promoted Hofmann-Martius rearrangement of hydroamination products toward hydroarylation products, resulting in high selectivity for hydroarylation products. It can be inferred that the weak acid sites of zeolite play a key role in forming hydroarylation products by  $\text{NH}_3$ -TPD. Importantly, the catalyst could be reused at least 10 times without apparent deactivation. This work may provide an important insight in development of heterogeneous catalyst for alkene hydroarylation.

### Declaration of Competing Interest

The authors declare that they have no known competing financial interests or personal relationships that could have appeared to influence the work reported in this paper.

### Acknowledgements

Financial supports from the NSFC (21925207), the Youth Innovation Promotion Association (2019409), the 'Light of West China' Program and Key Research Program of Frontier Sciences of CAS (QYDZJ-SSW-SLH051), are gratefully acknowledged. We thank Yan Guo (Lanzhou Institute of Chemical Physics, Chinese Academy of Sciences) and Chuanzhi Xu (Lanzhou Institute of Chemical Physics, Chinese Academy of Sciences) for helping us to perform the Py-IR and FT-IR analysis. We thank Dongmei Li (Lanzhou Institute of Chemical Physics, Chinese Academy of Sciences) and Li He (Lanzhou Institute of Chemical Physics, Chinese Academy of Sciences) for helping us to perform the XRD analysis. We thank Zhiqiang Shen (Lanzhou Institute of Chemical Physics, Chinese Academy of Sciences) for helping us to perform the SEM analysis. We thank Xiaoxue Hu (Lanzhou Institute of Chemical Physics, Chinese Academy of Sciences) for helping us to perform the HRMS

analysis. In addition, we thank the editor and reviewers for their constructive suggestions.

### Appendix A. Supplementary data

Supplementary data to this article can be found online at <https://doi.org/10.1016/j.jcat.2020.12.007>.

### References

- [1] Z. Dong, Z. Ren, S.J. Thompson, Y. Xu, G. Dong, Transition-Metal-Catalyzed C-H Alkylation Using Alkenes, *Chem. Rev.* 117 (2017) 9333–9403.
- [2] M. Nishiura, F. Guo, Z. Hou, Half-Sandwich Rare-Earth-Catalyzed Olefin Polymerization, Carbometallation, and Hydroarylation, *Acc. Chem. Res.* 48 (2015) 2209–2220.
- [3] Y. Yamamoto, Synthesis of heterocycles via transition-metal-catalyzed hydroarylation of alkynes, *Chem. Soc. Rev.* 43 (2014) 1575–1600.
- [4] M. Beller, O.R. Thiel, H. Trauthwein, Catalytic alkylation of aromatic amines with styrene in the presence of cationic rhodium complexes and acid, *Synlett* 2 (1999) 243–245.
- [5] L.L. Anderson, J. Arnold, R.G. Bergman, Proton-catalyzed hydroamination and hydroarylation reactions of anilines and alkenes: A dramatic effect of counteranions on reaction efficiency, *J. Am. Chem. Soc.* 127 (2005) 14542–14543.
- [6] I. Colomer, Hydroarylation of Alkenes Using Anilines in Hexafluoroisopropanol, *ACS Catal.* 10 (2020) 6023–6029.
- [7] S. Wang, G. Force, R. Guillot, J.-F. Carpentier, Y. Sarazin, C. Bour, V. Gandon, D. Lebeuf, Lewis Acid/Hexafluoroisopropanol: A Promoter System for Selective ortho-C-Alkylation of Anilines with Deactivated Styrene Derivatives and Unactivated Alkenes, *ACS Catal.* 10 (2020) 10794–10802.
- [8] S. Grelaud, P. Cooper, L.J. Feron, J.F. Bower, Branch-Selective and Enantioselective Iridium-Catalyzed Alkene Hydroarylation via Anilide-Directed C-H Oxidative Addition, *J. Am. Chem. Soc.* 140 (2018) 9351–9356.
- [9] A. Prades, R. Corberan, M. Poyatos, E. Peris, A Simple Catalyst for the Efficient Benzoylation of Arenes by Using Alcohols, Ethers, Styrenes, Aldehydes, or Ketones, *Chem. - Eur. J.* 15 (2009) 4610–4613.
- [10] I. Abdellah, A. Poater, J.-F. Lohier, A.-C. Gaumont, Au(i)-Catalyzed hydroarylation of alkenes with N, N-dialkylanilines: a dual gold catalysis concept, *Catal. Sci. Technol.* 8 (2018) 6486–6492.
- [11] X. Hu, D. Martin, M. Melaimi, G. Bertrand, Gold-Catalyzed Hydroarylation of Alkenes with Dialkylanilines, *J. Am. Chem. Soc.* 136 (2014) 13594–13597.
- [12] J. Chu, D. Munz, R. Jazsar, M. Melaimi, G. Bertrand, Synthesis of Hemilabile Cyclic (Alkyl)(amino)carbenes (CAACs) and Applications in Organometallic Chemistry, *J. Am. Chem. Soc.* 138 (2016) 7884–7887.
- [13] Y. Uchamaru, N-H activation vs. C-H activation: ruthenium-catalyzed regioselective hydroamination of alkynes and hydroarylation of an alkene with N-methylaniline, *Chem. Commun.* (1999) 1133–1134.
- [14] F. Schroeter, S. Lerch, M. Kaliner, T. Strassner, Cobalt-Catalyzed Hydroarylations and Hydroaminations of Alkenes in Tunable Aryl Alkyl Ionic Liquids, *Org. Lett.* 20 (2018) 6215–6219.
- [15] G.-Q. Liu, Y.-M. Li, Zinc triflate-catalyzed intermolecular hydroamination of vinylarenes and anilines: scopes and limitations, *Tetrahedron Lett.* 52 (2011) 7168–7170.
- [16] G. Song, G. Luo, J. Oyamada, Y. Luo, Z. Hou, ortho-Selective C-H addition of N, N-dimethyl anilines to alkenes by a yttrium catalyst, *Chem. Sci.* 7 (2016) 5265–5270.
- [17] W. Ma, G. Zhai, X. Hu, Y. Wu, Experimental and theoretical study on the cyclic (alkyl)(amino)carbene-copper catalyzed Friedel-Crafts reaction of N, N-dialkylanilines with styrenes, *Org. Biomol. Chem.* 18 (2020) 4272–4275.
- [18] J. Su, Y. Cai, X. Xu, Scandium-Catalyzed para-Selective Alkylation of Aromatic Amines with Alkenes, *Org. Lett.* 21 (2019) 9055–9059.
- [19] W. Zhu, Q. Sun, Y. Wang, D. Yuan, Y. Yao, Chemo- and Regioselective Hydroarylation of Alkenes with Aromatic Amines Catalyzed by  $[\text{Ph}_3\text{C}][\text{B}(\text{C}_6\text{F}_5)_4]$ , *Org. Lett.* 20 (2018) 3101–3104.
- [20] A.A.M. Lapis, B.A.D. Neto, J.D. Scholten, F.M. Nachtigall, M.N. Eberlin, J. Dupont, Intermolecular hydroamination and hydroarylation reactions of alkenes in ionic liquids, *Tetrahedron Lett.* 47 (2006) 6775–6779.

- [21] J.J. Brunet, N.C. Chu, O. Diallo, E. Mothes, Catalytic intermolecular hydroamination of alkenes - Beneficial effect of ionic solvents, *J. Mol. Catal. A: Chem.* 198 (2003) 107–110.
- [22] M. Perez, T. Mahdi, L.J. Hounjet, D.W. Stephan, Electrophilic phosphonium cations catalyze hydroarylation and hydrothiolation of olefins, *Chem. Commun.* 51 (2015) 11301–11304.
- [23] A.E. Cherian, G.J. Domski, J.M. Rose, E.B. Lobkovsky, G.W. Coates, Acid-catalyzed ortho-alkylation of anilines with styrenes: An improved route to chiral anilines with bulky substituents, *Org. Lett.* 7 (2005) 5135–5137.
- [24] H. Hart, J.R. Kosak, Mechanism of rearrangement of N-alkylanilines, *J. Org. Chem.* 27 (1962) 116–121.
- [25] K. Marcsekova, S. Doye, Hf-catalyzed hydroamination and hydroarylation of alkenes, *Synthesis* 1 (2007) 145–154.
- [26] L.T. Kaspar, B. Fingerhut, L. Ackermann, Titanium-catalyzed intermolecular hydroamination of vinylarenes, *Angew. Chem. Int. Ed.* 44 (2005) 5972–5974.
- [27] I. Fleischer, J. Pospech, Bronsted acid-catalyzed hydroarylation of activated olefins, *RSC Adv.* 5 (2015) 493–496.
- [28] C.K. Rank, B. Oezkaya, F.W. Patureau, HBF<sub>4</sub>- and AgBF<sub>4</sub>-Catalyzed ortho-Alkylation of Diarylamines and Phenols, *Org. Lett.* 21 (2019) 6830–6834.
- [29] Q. Zhang, J. Yu, A. Corma, Applications of Zeolites to C1 Chemistry: Recent Advances, Challenges, and Opportunities, *Adv. Mater.* 2002927 (2020).
- [30] Y. Li, L. Li, J. Yu, Applications of Zeolites in Sustainable Chemistry, *Chem* 3 (2017) 928–949.
- [31] V. Van Speybroeck, K. Hemelsoet, L. Joos, M. Waroquier, R.G. Bell, C.R.A. Catlow, Advances in theory and their application within the field of zeolite chemistry, *Chem. Soc. Rev.* 44 (2015) 7044–7111.
- [32] Z. Jin, L. Wang, E. Zuidema, K. Mondal, M. Zhang, J. Zhang, C. Wang, X. Meng, H. Yang, C. Mesters, F.-S. Xiao, Hydrophobic zeolite modification for in situ peroxide formation in methane oxidation to methanol, *Science* 367 (2020) 193–197.
- [33] Q. Sun, N. Wang, T. Zhang, R. Bai, A. Mayoral, P. Zhang, Q. Zhang, O. Terasaki, J. Yu, Zeolite-Encaged Single-Atom Rhodium Catalysts: Highly-Efficient Hydrogen Generation and Shape-Selective Tandem Hydrogenation of Nitroarenes, *Angew. Chem. Int. Ed.* 58 (2019) 18570–18576.
- [34] J. Wei, T. Wang, H. Liu, Y. Liu, X. Tang, Y. Sun, X. Zeng, T. Lei, S. Liu, L. Lin, Assembly of Zr-based coordination polymer over USY zeolite as a highly efficient and robust acid catalyst for one-pot transformation of fructose into 2,5-bis(isopropoxymethyl)furan, *J. Catal.* 389 (2020) 87–98.
- [35] B. Qiu, F. Jiang, W.-D. Lu, B. Yan, W.-C. Li, Z.-C. Zhao, A.-H. Lu, Oxidative dehydrogenation of propane using layered borosilicate zeolite as the active and selective catalyst, *J. Catal.* 385 (2020) 176–182.
- [36] J.M. Thomas, R. Raja, G. Sankar, R.G. Bell, Molecular sieve catalysts for the regioselective and shape-selective oxyfunctionalization of alkanes in air, *Acc. Chem. Res.* 34 (2001) 191–200.
- [37] S. Mohanty, A.V. McCormick, Prospects for principles of size and shape selective separations using zeolites, *Chem. Eng. J.* 74 (1999) 1–14.
- [38] N. Mizuno, M. Tabata, T. Uematsu, M. Iwamoto, Amination of 2-methylpropene over proton-exchanged ZSM-5 zeolite catalysts, *J. Catal.* 146 (1994) 249–256.
- [39] C.R. Ho, L.A. Bettinson, J. Choi, M. Head-Gordon, A.T. Bell, Zeolite-Catalyzed Isobutene Amination: Mechanism and Kinetics, *ACS Catal.* 9 (2019) 7012–7022.
- [40] S. Gao, X. Zhu, X. Li, Y. Wang, Y. Zhang, S. Xie, J. An, F. Chen, S. Liu, L. Xu, Thermodynamic study of direct amination of isobutylene to tert-butylamine, *Chin. J. Catal.* 38 (2017) 106–114.
- [41] S. Gao, X. Zhu, X. Li, Y. Wang, S. Xie, S. Du, F. Chen, P. Zeng, S. Liu, L. Xu, Direct amination of isobutylene over zeolite catalysts with various topologies and acidities, *J. Energy Chem.* 26 (2017) 776–782.
- [42] Y. Wu, T. Wang, H. Wang, X. Wang, X. Dai, F. Shi, Active catalyst construction for CO<sub>2</sub> recycling via catalytic synthesis of N-doped carbon on supported Cu, *Nat. Commun.* 10 (2019) 2599.
- [43] X. Dai, S. Adomeit, J. Rabeah, C. Kreyenschulte, A. Brueckner, H. Wang, F. Shi, Sustainable Co-Synthesis of Glycolic Acid, Formamides and Formates from 1,3-Dihydroxyacetone by a Cu/Al<sub>2</sub>O<sub>3</sub> Catalyst with a Single Active Sites, *Angew. Chem. Int. Ed.* 58 (2019) 5251–5255.
- [44] H. Wang, H. Yuan, B. Yang, X. Dai, S. Xu, F. Shi, Highly Selective N-Monomethylanilines Synthesis From Nitroarene and Formaldehyde via Kinetically Excluding of the Thermodynamically Favorable N, N-Dimethylation Reaction, *ACS Catal.* 8 (2018) 3943–3949.
- [45] Database of Zeolite Structures, <http://www.iza-structure.org/databases/>.
- [46] M.J. Frisch, Gaussian 16 Rev. C.01, in, Wallingford, CT, 2016.
- [47] P.J. Stephens, F.J. Devlin, C.F. Chabalowski, M.J. Frisch, Ab-initio calculation of vibrational absorption and circular-dichroism spectra using density-functional force-fields, *J. Phys. Chem.* 98 (1994) 11623–11627.
- [48] A.D. Becke, Density-Functional Thermochemistry. 3. The Role Of Exact Exchange, *J. Chem. Phys.* 98 (1993) 5648–5652.
- [49] A.D. Becke, A new mixing of hartree-fock and local density-functional theories, *J. Chem. Phys.* 98 (1993) 1372–1377.
- [50] C.T. Lee, W.T. Yang, R.G. Parr, Development of the colle-salvetti correlation-energy formula into a functional of the electron-density, *Phys. Rev. B* 37 (1988) 785–789.
- [51] T. Clark, J. Chandrasekhar, G.W. Spitznagel, P.V. Schleyer, Efficient Diffuse Function-augmented Basis Sets for Anion Calculations. III. The 3–21+G Basis Set for First-row Elements, Li–F, *J. Comput. Chem.* 4 (1983) 294–301.
- [52] Harihara, P.C., J.A. Pople, The Influence of Polarization Functions on Molecular Orbital Hydrogenation Energies, *Theor. Chim. Acta* 28 (1973) 213–222.
- [53] W.J. Hehre, R. Ditchfield, J.A. Pople, Self-Consistent Molecular Orbital Methods. XII. Further Extensions of Gaussian-Type Basis Sets for Use in Molecular Orbital Studies of Organic Molecules, *J. Chem. Phys.* 56 (1972) 2257–2261.
- [54] C.A. Emeis, Determination of integrated molar extinction coefficients for infrared-absorption bands of pyridine adsorbed on solid acid catalysts, *J. Catal.* 141 (1993) 347–354.
- [55] E.P. Parry, An infrared study of pyridine adsorbed on acidic solids characterization of surface acidity, *J. Catal.* 2 (1963) 371–379.
- [56] B. Hunger, H. Miessner, M. vonSzombathely, E. Geidel, Heterogeneity of Si-OH-Al groups in HNaY zeolites, *J. Chem. Soc. Faraday Trans.* 92 (1996) 499–504.
- [57] C.A. Fyfe, J.L. Bretherton, L.Y. Lam, Solid-State NMR Detection, Characterization, and Quantification of the Multiple Aluminum Environments in US-Y Catalysts by <sup>27</sup>Al MAS and MQMAS Experiments at Very High Field, *J. Am. Chem. Soc.* 123 (2001) 5285–5291.
- [58] J.A. van Bokhoven, D.C. Koningsberger, P. Kunkeler, H. van Bekkum, A.P.M. Kentgens, Stepwise Dealumination of Zeolite Beta at Specific T-Sites Observed with <sup>27</sup>Al MAS and <sup>27</sup>Al MQ MAS NMR, *J. Am. Chem. Soc.* 122 (2000) 12842–12847.
- [59] A.W. Hofmann, C.A. Martius, Methylierung der Phenylgruppe im Anilin, *Ber. Dtsch. Chem. Ges.* 4 (1871) 742–748.
- [60] S.-S. Gao, M. Garcia-Borras, J.S. Barber, Y. Hai, A. Duan, N.K. Garg, K.N. Houk, Y. Tang, Enzyme-Catalyzed Intramolecular Enantioselective Hydroalkoxylation, *J. Am. Chem. Soc.* 139 (2017) 3639–3642.
- [61] A.S.K. Hashmi, Dual Gold Catalysis, *Acc. Chem. Res.* 47 (2014) 864–876.
- [62] J.D. Egbert, C.S.J. Cazin, S.P. Nolan, Copper N-heterocyclic carbene complexes in catalysis, *Catal. Sci. Technol.* 3 (2013) 912–926.
- [63] K. Komura, R. Hongo, J. Tsutsui, Y. Sugi, Na-Y Zeolite as a Highly Active Catalyst for the Hydroamination of alpha, beta-Unsaturated Compounds with Aromatic Amines, *Catal. Lett.* 128 (2009) 203–209.